

**Low Frequency Airborne Sound Transmission in Buildings:
Modal Analysis**

M.D.C. Magalhaes and N.S. Ferguson

ISVR Technical Memorandum 864

July 2001



SCIENTIFIC PUBLICATIONS BY THE ISVR

Technical Reports are published to promote timely dissemination of research results by ISVR personnel. This medium permits more detailed presentation than is usually acceptable for scientific journals. Responsibility for both the content and any opinions expressed rests entirely with the author(s).

Technical Memoranda are produced to enable the early or preliminary release of information by ISVR personnel where such release is deemed to be appropriate. Information contained in these memoranda may be incomplete, or form part of a continuing programme; this should be borne in mind when using or quoting from these documents.

Contract Reports are produced to record the results of scientific work carried out for sponsors, under contract. The ISVR treats these reports as confidential to sponsors and does not make them available for general circulation. Individual sponsors may, however, authorize subsequent release of the material.

COPYRIGHT NOTICE

(c) ISVR University of Southampton All rights reserved.

ISVR authorises you to view and download the Materials at this Web site ("Site") only for your personal, non-commercial use. This authorization is not a transfer of title in the Materials and copies of the Materials and is subject to the following restrictions: 1) you must retain, on all copies of the Materials downloaded, all copyright and other proprietary notices contained in the Materials; 2) you may not modify the Materials in any way or reproduce or publicly display, perform, or distribute or otherwise use them for any public or commercial purpose; and 3) you must not transfer the Materials to any other person unless you give them notice of, and they agree to accept, the obligations arising under these terms and conditions of use. You agree to abide by all additional restrictions displayed on the Site as it may be updated from time to time. This Site, including all Materials, is protected by worldwide copyright laws and treaty provisions. You agree to comply with all copyright laws worldwide in your use of this Site and to prevent any unauthorised copying of the Materials.

UNIVERSITY OF SOUTHAMPTON
INSTITUTE OF SOUND AND VIBRATION RESEARCH
DYNAMICS GROUP

**Low Frequency Airborne Sound Transmission in
Buildings : Modal Analysis
(Computational Experiments)**

by

M.D.C. Magalhaes and N.S. Ferguson

ISVR Technical Memorandum No: 864

July 2001

Authorized for issue by
Dr M.J. Brennan
Group Chairman

Summary

This *memorandum* describes a general theoretical model for coupled interior sound fields, which are created by excitation due to a noise source, in one source room.

The pressure is explicitly described in terms of the acoustic and structural modal parameters and structural-acoustic modal coupling coefficients, which have a large effect on the noise reduction values at the resonance frequencies.

Numerical predictions are presented considering the governing equations for general acoustic-structural coupled systems. These procedures were evaluated by using a computer program, which has been developed during the course of this study in MATLAB. Simulations show the effect on noise reduction of several configurations for a flexible partition, at different geometric arrangements in the common wall, and for various room geometry and properties (i.e. size and absorbing walls).

In addition, transmission loss for the models examined, obtained via modal analysis, are compared with those obtained by conventional approaches.

Contents

1 Introduction	1
2 Theoretical Background of the Sound Transmission Mechanism	5
3 Theoretical Model for the Fluid-Structural Coupled System	12
4 Numerical Results	17
5 Conclusions	23
6 References	24
7 Tables	26
8 Figures	29
9 Appendix – List of symbols	32

1 Introduction

The initial aim of this work is to improve the understanding of the noise transmission phenomenon in buildings, at low frequencies, using an acoustic-structural coupled model (room-plate-room). The model is represented by sets of integro-differential modal equations of motion. The low-frequency range is defined as the modal domain, for which the associated conservative system has a low modal density [1]. The effects of low-frequency noise have been of particular concern because many kinds of structures have proved inefficient in attenuating low-frequency noise, whereas other frequencies are less problematic or can be analysed successfully using existing techniques.

The frequency range of human hearing is considered to be between 20 Hz and 20,000 Hz. However, it has been shown that humans can perceive sounds below 20 Hz (if one considers a signal that has a high sound pressure level) and also detect it through their bodies [2].

Sound insulation requirements for buildings depend on the listener's activities and also on the background noise, which may be considered as part of the work or home environment. The problem of sound transmission has become an important subject in noise control in buildings. Usually a noise is communicated to rooms via many different paths. Moreover, noise sources may be elsewhere in the building and/or outside the building. In airborne sound transmission the noise originates in the air. This work considers the insulation provided by a single-leaf partition for airborne sound. The greater the sound insulation provided by a partition, the higher its sound reduction index.

The problem of calculating the sound transmission between rooms has been investigated over many years [3-8]. The three main approaches have been the conventional Wave Approach, Modal Analysis and Statistical Energy Analysis.

In the Wave Approach, infinitely extended panels are used as sound transmission models. For the first group of these models, boundary effects are neglected and the walls are assumed to be homogeneous and to have no leaks. The so-called mass law behaviour has

been successfully applied to many situations where frequencies are well below the coincidence frequency. However, the assumptions provided are unsatisfactory in a large number of real panels whose dimensions are less than or equal to the wavelength of the incident sound wave. In addition, the geometry of the system is not taken into account and, at low frequencies, the assumption of an incident diffuse field is incorrect.

Alternatively, Modal Analysis allows the geometric parameters of the system to be incorporated into the models and subsequent predictions. The frequency response of a finite-system normally has peaks and dips, due to the resonance phenomenon which involves modal behaviour and fluid-structure spatial coupling of plate and room modes. The method also permits calculation of the radiation of small structures at low frequencies, within a reasonable operational running time.

Finally, Statistical Energy Analysis considers the power flow balance between linear coupled systems. Statistical Energy Analysis (SEA) has been applied to solve some problems of noise transmission in buildings, aircraft, cars, etc. The estimates of subsystem energies are obtained on the basis of known 'a priori' values for the loss factors, coupling loss factors and the power inputs [9].

There has also been further investigation [3] with work closely related to this research. The transmission of a reverberant sound field through a rectangular baffled partition, by means of a mode expansion method, was analyzed. According to the formulae derived, valid for non-resonant transmission, the problem was well predicted provided that the mass of the partition was significant. In these conditions, it was observed that the imaginary part of the fluid wave impedance is significantly greater than its real part. Therefore it ensured that the forced vibration, or *mass law* contribution, dominated the transmission factor. A detailed review in order to investigate acoustic-structural coupled systems was also presented. A theoretical model was developed for arbitrary wall motions using Green's Theorem. From the point of view of applications, a simplified formulation was also presented for sound level predictions in terms of acoustic and structural parameters.

The effects of panel boundaries on sound transmission, including a comparison with an infinite panel, were discussed in ref. [7]. A simple two-dimensional model was used for evaluating the sound transmission characteristics of finite panels. The analysis of the transmission, through a baffled plate of finite width and infinite length, was conducted rigorously. The effects of panel size were verified in regions below, above and at the critical frequency. Estimates of averaged response over a particular frequency range have also been presented. Sound transmission in the diffuse field was hence obtained via numerical direct-integration.

More recently Osipov et al [10] evaluated some numerical examples in order to verify the influence of the dimensions of rooms and partitions on the transmission phenomenon. The problem of low frequency sound insulation in buildings was identified as a growing research area. In their work, three distinct theoretical models (infinite plate theory and modal analysis for a baffled partition and for a room-plate-room system) were compared with experimental results.

Other alternatives have also been considered, e.g. the Finite Element Method [11,12], to predict sound insulation considering the effect of partition edge conditions at low frequencies. Furthermore, an interesting approach, considering impedance-mobility representations, was adopted and applied to many sound and vibration problems [5].

In summary, a vast amount of research concerning acoustic-structural coupling has been published. The literature survey has shown that a large amount of work has been performed in the analysis of sound insulation phenomena. However, the combined effect of parameters in noise control in buildings, in particular the sensitivity to geometry, has not yet been fully explored.

With a point noise source placed in either of the rooms, the aim is to predict the noise reduction of the system due to resonant coupling involving modal behaviour, spatial fluid-structural coupling and non-resonant contributions. Moreover, some interesting

results in terms of transmission efficiency are examined when the weight of the partition is increased.

The transmission of sound from rooms attached to corridors can also be predicted in this research. An analysis of the position or arrangement of a flexible panel in the common wall, considering that all other parts of the common wall are rigid, is predicted. The results of analyses were converted to an approximate one-third-octave-band spectrum to make comparisons with other data possible.

Finally, a general discussion, based on the findings of the results obtained, is presented, with some observation concerning potential improvements that can be considered.

2 Theoretical Background of Sound Transmission Mechanism

The mechanism of sound transmission may be characterised as a radiated sound field from an elastic partition itself excited by a sound field in a source room. The response of thin plates to localised excitation results in free bending waves. Those waves interact with plate edges producing sound power radiation. In addition, another contribution to the total radiated noise comes from the in phase vibration of the plate in the vicinity of the excitation point. Alternatively, when a sound wave is incident upon a partition, the response, which is frequency dependent, is also dependent on the radiation impedance of the modes of the partition. Thus, the air on the other side of the plate is excited, and a sound wave is then propagated into the receiving volume.

In general, the sound transmission theory for uniform and unbounded panels has widely been used to approximate the sound transmission loss of a bounded panel in a baffle. Of course, some assumptions, such as the random-incidence field over the partition, as well as a limited frequency range (in which the acoustical wavelength is smaller than the plate size), have been considered.

A transmission efficiency parameter τ defined as the ratio of transmitted to incident power, is given by

$$\tau = \frac{w_{trans}}{w_{inc}} \quad (2.1)$$

where

w_{trans} is the transmitted sound power;

w_{inc} is the sound power incident on the source side of the test partition.

A classical index, known as Transmission Loss (TL), in some countries, or Sound Reduction Index (SRI) has also been defined as

$$SRI = 10 \log_{10} (1/\tau) \text{ (dB)} \quad (2.2)$$

A finite-size panel (bounded rectangular plate in a baffle) is a more realistic model than the infinite one described above. The transmission is characterized by boundary effects, which lead to the formation of standing-wave modes. Although simply supported edges will be

considered in this work for reason of simplicity, complex boundary conditions have also been discussed in the literature as well.

An infinite set of *in vacuo* modes, represented by a functional basis, which is assumed to be the solution of the equation of motion for the flexible plate, is given by

$$\phi_p(z, y) = \sin(k_z z) \sin(k_y y) \quad (2.3)$$

This basis function, used in the expansion for the panel deflection, must not only ensure a vanishing normal displacement on the contour of the panel but also respect the panel boundary conditions. It satisfies the boundary conditions and the equation of motion as long as

$$k_b^2 = k_{pr}^2 = k_z^2 + k_y^2 = \left(\frac{r\pi}{L_z} \right)^2 + \left(\frac{s\pi}{L_y} \right)^2 \quad (2.4)$$

where $(k_{pr})^2$ – *in vacuo* eigenvalues

L_z – length of the panel;

L_y – height of the panel;

r, s – panel mode;

Furthermore, the infinite set of *in-vacuo* modes, defined by Equation 2.3, represents a set of orthogonal functions, which satisfy the following orthogonality relationships

$$\begin{aligned} \int_S \phi_q^T m(r_s) \phi_p dS &= \begin{cases} 0 & \text{if } p \neq q; \\ \Lambda_p & \text{if } p = q. \end{cases} \\ \int_S D \nabla^2 \phi_q \nabla^2 \phi_p dS &= \begin{cases} 0 & \text{if } p \neq q; \\ \omega_p^2 \Lambda_p & \text{if } p = q. \end{cases} \\ \Lambda_p &= \int_S m(r_s) \phi_p^2 dS \end{aligned} \quad (2.5)$$

where $m(r_s)$ = mass per unit area of the partition;

Λ_p = modal-generalized mass;

ω_p = *in vacuo* natural frequencies of the plate;

D = bending stiffness of the partition;

∇^2 = two-dimensional Laplace operator;

p, q = mode identifiers.

To determine the far-field sound intensity radiated and consequently the transmission, the sound field generated by a harmonic vibrating surface has to be evaluated. The sound field generated by a baffled harmonic vibrating surface S at position r in the fluid is given by a particular form of Kirchhoff-Helmholtz integral equation, which is termed the Rayleigh Integral [6]. The key function of this problem is to obtain the difference of pressure between both sides of the panel.

The total surface pressure is hence the summation of the *blocked pressure* and the radiated pressure. This *blocked pressure* is defined as the summation of the incident field and the scattered field produced if the plate were rigid (infinite mechanical impedance). The radiated pressure is the field produced as a result of the elasticity of the plate, and subsequently motion producing sound radiation.

The equation of motion of an elastic partition in the absence of sound radiation is given as

$$D\{\nabla^4[w(z,y,\omega)] - k_b^4 w(z,y,\omega)\} = p_{bL}(z,y,\omega) \quad (2.6)$$

and

$$w(z,y,\omega) = \sum_p w_p \phi_p \quad (2.7)$$

$$p_{bL} = 2 \int_S p_o \phi_p dS \quad (2.8)$$

where p_{bL} – modal-generalized force;

$p_o(z,y,\omega)$ – incident field amplitude of pressure;

ϕ_p – basis function;

D – bending stiffness;

∇^4 – square of the Laplace operator;

k_b – wavenumber of the free-bending wave;

$w(z,y,\omega)$ – normal displacement of the plate surface;

In equation 2.6 the time term $e^{j\omega t}$ is suppressed, as well as the damping influence. After solving this equation, the power radiated into a half-space, due to the plate vibration, can be obtained by

$$\Pi(\omega) = \frac{1}{2} \int_S \operatorname{Re} \left[p(z, y, 0) \dot{w}(z, y, 0)^* \right] dS \quad (2.9)$$

where $\Pi(\omega)$ = total power radiated.

The real part of the radiation impedance (radiation resistance) may also be defined for the p mode of the plate as

$$R_p = \frac{\Pi(\omega)}{\frac{1}{2} \left\langle \left| \dot{w}_p \right|^2 \right\rangle} \quad (2.10)$$

where the spatial-average mean-square normal velocity is given by

$$\frac{1}{2} \left\langle \left| \dot{w}_p \right|^2 \right\rangle = \frac{1}{2S} \int_S \left| \dot{w}_p \right|^2 dS \quad (2.11)$$

Finally, the full problem, considering fluid loading in the equation of motion, can be solved. Thus, one may obtain some results in terms of coupled *in vacuo modes*.

Let $p(x, y, z, t)$ be regarded as small amplitude perturbation (acoustic pressure variation) from its equilibrium value. The wave equation which results from the linear acoustic equations is given by [14]

$$\begin{aligned} \nabla^2 p - \frac{1}{c^2} \frac{\partial^2 p}{\partial t^2} &= 0 \\ \frac{\partial p}{\partial n} &= 0 \text{ on the rigid walls of the room;} \\ \frac{\partial p}{\partial n} &= -\rho_0 \frac{\partial^2 w}{\partial t^2} \text{ on the flexible partition} \end{aligned} \quad (2.12)$$

where w = the displacement of the flexible partition in the normal direction (positive outward).

The steady-state solution is obtained through the Fourier Transform of the time domain wave equation, yielding the Helmholtz Equation

$$\nabla^2 \bar{p} + k^2 \bar{p} = 0 \quad (2.13)$$

If \bar{p} is expressed as an expansion of eigenfrequencies for the room, corresponding to the resonances of a rigid boundary space, a Green's function can be obtained satisfying the same condition [6]

$$\begin{aligned} \frac{\partial G(\mathbf{r}|\mathbf{r}_o)}{\partial n} &= 0 \quad \mathbf{r} \in S_r \\ \nabla^2 G(\mathbf{r}|\mathbf{r}_o) + k^2 G(\mathbf{r}|\mathbf{r}_o) &= -\delta(\mathbf{r} - \mathbf{r}_o) \\ G(\mathbf{r}|\mathbf{r}_o) &= \sum_n A_n \Psi_n(\mathbf{r}) \end{aligned} \quad (2.14)$$

where S_r is the surface area of the rigid walls;

$\delta(\mathbf{r} - \mathbf{r}_o)$ is the three-dimensional Dirac Delta function representation of a point source.

$G(\mathbf{r}|\mathbf{r}_o)$ is the solution (Green's function) of equation 2.14;

Ψ_n = acoustic-pressure mode shape of the room.

The spatial form for the three-dimensional eigenfunctions Ψ_n , corresponding to the natural frequency ω_n of the rigid-walled space, may be defined as

$$\Psi_n = \cos\left(\frac{n_x \pi \cdot x}{L_x}\right) \cos\left(\frac{n_y \pi \cdot y}{L_y}\right) \cos\left(\frac{n_z \pi \cdot z}{L_z}\right) \quad (2.15)$$

This set of modes satisfies the relationship

$$\begin{aligned} \int_V \Psi_m \Psi_n dV &= \begin{cases} 0 & \text{if } m \neq n; \\ \Lambda_n & \text{if } m = n. \end{cases} \\ \Lambda_n &= \int_V \Psi_n^2(x, y, z) dV \end{aligned} \quad (2.16)$$

where Λ_n = mean-squared volume averaged.

Since ψ_n is an eigenfunction of the room, it has a correspondent eigenvalue k_n which must satisfy

$$\nabla^2 \Psi_n + k_n^2 \Psi_n = 0 \quad (2.17)$$

Therefore, using the previous relationships, equation (2.14) can be written as

$$\sum_n A_n (-k_n^2 + k^2) \Psi_n = -\delta(r - r_o) \quad (2.18)$$

Multiplying each side of equation (2.18) by $\psi_m(x, y, z)$ and integrating over the volume of the room one has [6]

$$A_n = \frac{\Psi_n(x_o, y_o, z_o)}{\Lambda_n(k_n^2 - k^2)} \quad (2.19)$$

A review of velocity-potential concepts is also important if one uses an alternative formulation. For an inviscid-flow (viscous effects are neglected), low-speed flows are irrotational [15]. This means that

$$\begin{aligned} \text{If } \nabla \times \mathbf{V} = 0 \quad \text{then } \mathbf{V} = \nabla \Phi \\ u_x = \frac{\partial \Phi}{\partial x}; \quad u_y = \frac{\partial \Phi}{\partial y}; \quad u_z = \frac{\partial \Phi}{\partial z}; \end{aligned} \quad (2.20)$$

where \mathbf{V} - fluid velocity;

(u_x, u_y, u_z) - fluid velocity components;

Φ - scalar function termed velocity potential.

Therefore, the velocity potential function allows one to obtain all other acoustic parameters through the relationship

$$p = -\rho_o \frac{\partial \Phi}{\partial t} \quad (2.21)$$

The equations defined above, describing uncoupled modal models, can therefore be used to develop an acoustic-structural coupled model in order to predict the sound insulation.

Beranek [16] has suggested a simple formulation for SRI, in which the sum of the radiation efficiency (in dB) of the sound-forced finite plate plus 3 dB, is subtracted from the value obtained by normal incidence mass-law. In this approximation, the radiation efficiency used was originally defined in ref. [17].

The transmission loss for a baffled panel has also been studied by Leppington [18,19]. His predictions have been considered an improvement on previous theories. A random field was considered as an infinite sum of uncorrelated plane-waves impinging on the finite-panel surface. In contrast, an assumption usually adopted was to consider the random field as a diffuse field, neglecting the presence of the boundaries. Moreover, the transmission problem was described in terms of two distinct mechanisms. The first one is dominant at the region of the spectrum above the critical frequency, where free bending waves interact to cause resonance. In this frequency range, the partition is a good radiator. In fact, its radiation efficiency is always greater than or equal to unity. For the second mechanism, free bending waves are not generated, and in this frequency range (below the critical frequency), the partition behaviour is as a poor radiator.

In summary, one can consider the transmission phenomenon as a summation of the non-resonant or forced transmission, and the resonant transmission. In numerous cases, the resonant transmission for frequencies below the critical frequency of the partition is rather important [18,19].

3 Theoretical Model for the Fluid-Structural Coupled System

In the present analysis, the room-panel-room system is selected as the fundamental model, which may represent a real situation in a building. The physical mechanisms involved in the control of sound transmission in buildings can hence be evaluated. As mentioned previously, the analytical modal model adopted [6] is based on a set of integro-differential equation formulation of the interaction between a flexible plate and enclosed fluids. The acoustic and the structural fields are expressed in terms of their uncoupled modes by means of differential equations for each mode. Therefore, the structural motion has been expressed as a summation over the response in the *in vacuo* natural modes driven by fluid loading. The acoustic-field of the rigid-walled rectangular rooms has been determined by the summation of the acoustic modes over the fluid volume. In fact, these acoustic modes were excited by a generalized volume velocity source (whose value was set equal to unit).

Interaction analysis was conducted when two fluid volumes connected by a thin plate were excited by a point monopole source placed in one of them. In addition, solid surfaces, which bounded volumes of air V_1 and V_2 , were considered. The response of the coupled system to a forcing harmonic function, can be represented in terms of the uncoupled modes of both rooms and the uncoupled panel modes as [6]

$$\begin{aligned}
 \ddot{\Phi}_{n1} + \beta_{n1} \dot{\Phi}_{n1} + \omega_1^2 \Phi_{n1} &= (c^2 S / \Lambda_{n1}) \sum_p \dot{w}_p C_{n1p} - c^2 Q_{n1} / \Lambda_{n1} \\
 \ddot{w}_p + \beta_p \dot{w}_p + \omega_p^2 w_p &= -(\rho_o S / \Lambda_p) \sum_{n1} \dot{\Phi}_{n1} C_{n1p} + (\rho_o S / \Lambda_p) \sum_{n2} \dot{\Phi}_{n2} C_{n2p} \\
 \ddot{\Phi}_{n2} + \beta_{n2} \dot{\Phi}_{n2} + \omega_2^2 \Phi_{n2} &= - (c^2 S / \Lambda_{n2}) \sum_p \dot{w}_p C_{n2p}
 \end{aligned} \tag{3.1}$$

where indices n_1 , n_2 , and p refer to source room, receiver room and panel modes respectively.

According to Fahy F.J. [6], the correct convergence of the modal pressure on the partition surface is obtained due to the Gibb's phenomenon.

The spatial structural-acoustic coupling coefficient C_{np} , assuming simply-supported edges for the partition, is defined by

$$\frac{1}{S} \int_S \psi_n \cdot \phi_p dS \quad (3.2)$$

where

Q = generalized volume velocity,

Φ = modal velocity potential amplitude,

β = generalized modal-damping coefficient.

The numerical determination of the eigenvalues and eigenfunctions for the coupled system has been obtained using a dynamic matrix formulation for the problem. The analysis was applied to the free vibration problem of the coupled room-panel-room system in order to determine the eigenvalues and eigenvector, and also to the forced-vibration problem.

An average absorption coefficient was firstly considered in terms of the corresponding modal loss factor. In equation 3.1, the effect of the absorbing material has been approximated by equivalent damping factors β_n . Then spatial averaged mean square pressures, whose amplitudes were obtained directly from the linear plate equation and velocity potential equations for the rooms, are also calculated.

The transmission parameters obtained from the modal room-panel-room model, finite-panel predictions [3,18] and a classical approach can be compared graphically as a function of frequency.

The ‘loading’ applied to the source room is represented by the generalized source strength as [6]

$$Q_n = \int_V q_o \Psi_n(x, y, z) dV \quad (3.3)$$

where

q_o – distribution of source volume velocity per unit volume.

Neglecting the cross-modal coupling terms introduced by the absorption on the boundary of the volume, and assuming that a single room mode is dominant, the approximation for the generalized modal damping may be given as [20]

$$\beta_n = \left(\frac{\rho_o c^2}{\Lambda_n} \right) \int_A \frac{\psi_n \psi_n}{z_a} dA \quad (3.4)$$

The real specific acoustic impedance z_a for the wall surfaces, lined by a soft porous material, on the assumption of light damping, with its reactive part not altering the resonance frequency significantly, may be approximated by [18]

$$z_a = \frac{8 \rho_o c}{\alpha} \quad (3.5)$$

where α is the diffuse absorption coefficient for an internal surface A of the room.

This assumption is valid when [16]

$$\left| \operatorname{Re} \left(\frac{\rho_o c}{z_a} \right) \right| \ll 1 \quad (3.6)$$

$$\left| \operatorname{Im} \left(\frac{\rho_o c}{z_a} \right) \right| \ll 1 \quad (3.7)$$

The pressure field, which acts on the partition surface, may be expressed in the acoustic and structural basis. At any particular point on the plate, which is located in the plane $x = x_o$, the pressure values obtained from either the acoustic or structural basis function expansion are equal. Therefore, the generalized force exerted on the p^{th} plate mode by the n^{th} acoustic mode of the receiving room is expressed as [13]

$$\begin{aligned} \bar{p}_R &= \frac{C_{n2p}}{\Omega_p} p_{n2} \\ \Omega_p &= \frac{1}{S} \int_S \phi_p^2 dS \end{aligned} \quad (3.8)$$

where

$$p_{n2} \equiv p_{n2}(x_o, t) = \bar{p}_{n2} \cos \left(\frac{n_x \pi x_o}{L_x} \right);$$

\bar{p}_{n2} = the receiving room generalized modal pressure;

C_{n2p} = geometrical coupling coefficients between the panel modes and the receiving room modes;

\bar{p}_R = generalized pressure over the partition in the receiving-room;

ϕ_p = *in vacuo* plate modes (see equation 2.3).

The spatial-average mean normal intensity transmitted by the panel is defined as [16]

$$\langle I_R \rangle = \frac{1}{2S} \int_S \text{Re}\{p_R v^*\} dS \quad (3.9)$$

where

v^* = the complex conjugate of the particle velocity on the panel surface;

p_R = pressure over the partition in the receiving-room.

As the particle velocity is equal to the normal velocity of the panel on its surface, equation (3.9) can be evaluated using the orthogonality property of the plate modes (equation 2.5) as

$$\langle I_R \rangle = \frac{1}{2} \sum_p \text{Re}\left\{\bar{p}_R \dot{w}_p^*\right\} \Omega_p \quad (3.10)$$

where

\dot{w}_p = generalized normal panel velocity.

Therefore, according to equation 3.8 the transmitted intensity can be expressed as

$$\langle I_R \rangle = \frac{1}{2} \sum_p \sum_n \text{Re}\left\{C_{n2p} \cdot p_{n2} \cdot \dot{w}_p^*\right\} \quad (3.11)$$

The mean sound intensity incident on the partition is approximated by

$$\langle I_i \rangle = \frac{1}{8\omega\rho_o} \sum_{m=0}^{nm1} \sum_{n=0}^{nm1} \text{Re}\{p_{n1} \cdot C_{mni} \cdot k_x \cdot p_{n1}^*\} \quad (3.12)$$

and

$$C_{mni} = \frac{1}{S} \int_S \cos(k_{zn}z) \cos(k_{yn}y) \cos(k_{zm}z) \cos(k_{ym}y) dz dy \quad (3.13)$$

$$k_x = \sqrt{k^2 - k_n^2} \quad (3.14)$$

$$k_n = \sqrt{k_{yn}^2 + k_{zn}^2} \quad (3.15)$$

where

$nm1$ = total number of modes considered in the source room.

k_{yn} ; k_{zn} – wavenumber components in the y and z directions respectively;

p_{nl} – reverberant sound field amplitude in a source room due to a point source having unit volume velocity [16];

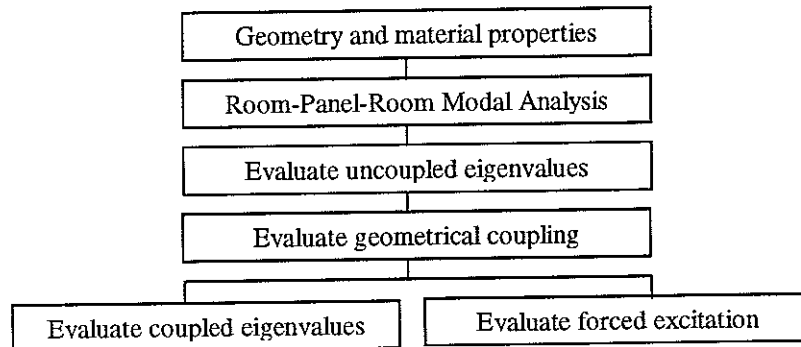
Finally, one can evaluate the SRI (Sound Reduction Index) and the NR (Noise Reduction) as

$$SRI = 10 \log_{10} \left(\frac{\langle I_i \rangle}{\langle I_R \rangle} \right) \quad (3.16)$$

$$NR = 10 \log_{10} \left(\frac{\langle |p_{n1}|^2 \rangle}{\langle |p_{n2}|^2 \rangle} \right) \quad (3.17)$$

NR is dependent upon the absorption in the room whilst it is assumed that SRI is independent of the room absorption.

The theoretical routines were developed according to the chart below:



4 Numerical Results

4.1 – General description of models

The models adopted comprised of three subsystems: a source room, a common wall and a receiving room (Figure 1). The source room was defined as an acoustic volume excited by a broadband acoustic point source placed in a specific position, and the receiving room was defined as the acoustic volume connected to the source volume through a common rigid wall with a flexible elastic partition. The results obtained from numerical examples provided important information about the sensitivity of the Sound Reduction Index to some parameters, such as different positions for the flexible panel, not normally considered in the design of buildings. The geometric dimensions of the models are shown in Figures 2a and 2b. Predicted incident intensity (actual field) on the flexible common wall was used for the SRI calculations rather than assuming a diffuse sound field assumption. Nevertheless, the actual field values tend to those for the diffuse field as the frequency increases. Spatial averaged mean square pressures were obtained directly from the linear Euler's equation.

The system properties are described as follows. For a partition made of plasterboard material, a value of $\nu = 0.24$ and $E = 2.12E9(N/m^2)$ were assumed for the Poisson's ratio coefficient and Young's Modulus respectively. Also a density value of $\rho_s = 806 (kg/m^3)$ and a thickness of 0.025 m [21] were assumed for the material. Therefore, the assumption of only pure bending waves propagating in the panel remains valid. When varying the other parameters, the receiving and source room surfaces were considered as being covered by a soft material with a constant modal frequency-average absorption coefficient. The material properties considered here were extracted from ref. [16] and [21]. The absorption coefficients for the volume surface were chosen as an averaged value of 0.05 (live rooms) over the whole frequency range. Nevertheless, as mentioned previously, an important approximation considered here is that the mode functions to be used have been chosen as the mode shapes of a volume bounded by rigid walls.

Moreover, the acoustic source strength applied to the source room was a unit volume velocity ($1 m^3/s$). The source was placed at position 1 (corner of the room) for all simulations other than that for analyzing the influence of source position on SRI.

The transmission loss parameters obtained from the modal and classical approaches [16,18] were compared graphically as a function of frequency. It was verified [18] that Leppington's prediction is the one, which approaches the values obtained via infinite theory when the non-resonant transmission is characterized.

The results are organized as follows. In section 4.2, the calculated values of the acoustic and structural natural frequencies are presented. They are also compared with the coupled and damped coupled natural frequencies. In section 4.3, normalized spatial coupling coefficients illustrate the contributions of modes at the frequency range of interest (Figures 4a-4b). In section 4.4, the influence of depth of source room (in both models) on SRI is described. The area of absorption surfaces remained the same. In real buildings, the flat floor is normally divided into rooms, with the same height. The influence of panel positions (Figures 6a –6b) on SRI is discussed in section 4.5. Three and five different positions were considered for models 1 and 2 respectively. The results are compared with Leppington's prediction [11] and the field-incidence mass law theory [6]. In section 4.6, the influence of increasing absorption on the walls of receiving room is assessed (Figures 7a-7b). Finally, the effects of altering noise source location (Figures 8a-8b) in the source room are also discussed in section 4.7.

4.2 –Acoustic and Structural modes of the system

It may be verified that the location of the resonance peaks and dips for the harmonic forced response approximately coincided with the eigenvalues obtained from the coupled analysis. For room dimensions of $2 \times 2 \times 5 \text{ m}^3$ and $2 \times 2 \times 2 \text{ m}^3$, 90 and 39 modes were respectively obtained (see table 1) for a frequency range up to 300 Hz. For panel dimensions of $2 \times 5 \text{ m}^2$, $2 \times 2 \text{ m}^2$ and $1 \times 1 \text{ m}^2$, a total of 110, 41 and 8 modes were considered respectively for the same frequency range (see table 2).

The absorbing material on the room walls and the internal loss factor of the plate had little effect on shifting the eigenfrequencies, whereas the geometrical coupling coefficients played a leading role. It can be confirmed by the natural frequency values obtained for the first 10 modes of the system (see table 3). For instance, the average difference between the coupled and damped coupled natural frequencies for the large panel ($2 \times 5 \text{ m}^2$) was irrelevant.

Another important point is that the fundamental natural frequency of the panel ($1 \times 1 \text{ m}^2$) was greater than the lowest natural frequency of the source room (34 Hz). Hence, the corresponding panel mode contributed with an equivalent stiffness. The coupled natural frequency of the system was about 32.9 Hz (see table 4 and 5).

Some simplifications, considering ‘poor’ spatial coupling of higher order modes, have been suggested by some authors [8]. Although this option was not considered here, table 4 and 5 show that generally the higher the order of the coupled modes, the less significant the influence of different panel positions.

4.3 – Coupling coefficients

Considering that the structural-acoustic coupling characteristics of the room-plate-room model are quite complex, all modes below 300 Hz, including non-resonant contributors, have been considered. Even though there were many ‘weak coupling coefficients’ (Figures 4a and 4b), their summation might be significant to the total coupling. The geometrical coupling values were obtained according to equation 3.2. When an acoustic wave-number \mathbf{k} coincided with a structural one (\mathbf{k}_p), the geometrical coupling coefficients \mathbf{C}_{np} were set to zero for the whole wall problem ($m_1 = r_1$ and/or $n_1 = p_1$). However, for a flexible panel in the common wall, \mathbf{C}_{np} were surely dependent upon panel position and size. These coefficients were normalized by their maximum absolute value in order to compare both models. The peak value is $4/\pi^2$ for the coupling between uniform pressure acoustic mode across the panel and its fundamental mode.

The results show that strongly excited structural modes generate low values for the SRI, which are determined by the structural-acoustic modal coupling coefficients as well as the damping factors.

For a panel located at the centre of common wall, a reduced coupling condition was found. According to results, the relationship between uncoupled structural and acoustic mode shape functions showed large values at the lower order modes.

4.4 - Influence of source room dimensions on the SRI parameter

The depth of the source room (x direction) was modified from 2 m to 5 m in both models. The results (figure 5a and 5b) show that for model 1 the SRI value varies by about 15 dB and for model 2 it varies by about 10 dB. The difference between the values reduces at higher frequencies than those which are being considered here. Similar rooms are strongly coupled at the interface (common wall) due to their identical acoustic mode shapes and resonance frequencies. Two types of acoustic modes, the panel-controlled mode and the room-controlled mode, appear distinctly at low frequencies. The lowest SRI value corresponds to a panel-controlled resonance frequency of the system. Alternatively, for a system composed of rooms of different volumes (model 2), a higher sound insulation is obtained. These situations might also be described in terms of the acoustic impedance mismatching of the rooms.

4.5 - Influence of Panel Position on the SRI parameter

The sensitivity of the SRI relative to the flexible panel positions, with the rest of the common wall rigid, is shown in figures 6a and 6b compared to Leppington's prediction [11] and field incidence mass law [6]. The latter two agree probably because the resonant terms of the equation were negligible compared to the non-resonant contribution, due to the low radiation efficiency of the corresponding modes. The transmission behaviour becomes complex and dependent on the panel position.

For model 1, a distinct dip in the SRI was verified at about the resonance frequency of the room (34 Hz). It is known that at panel-controlled resonance, SRI is not dependent on room impedance, but upon geometrical coupling factors. At low frequencies, the spatial distribution of room modes varies mainly along preferential directions (e.g. the z axis direction). Hence, below 100 Hz, the SRI curve (figure 6a) exhibits distinct dips for the panel at the corner, where the tangential modes in the receiving room were fully excited. For the partition in the middle of the common wall, higher SRI values are obtained due to the very weak excitation of the anti-symmetric source room modes. When the frequency increased, oblique modes tended to be dominant in the rooms and the difference between the positions became less important on sound insulation.

For model 2, the effects of panel position were also significant on noise insulation only at very low frequencies. However, the variation of SRI values was less pronounced than that for the model 1, due to the mismatch of the resonance frequencies of both rooms. Above about

170 Hz, the wavelength of the waves assumed values less than the heights of the rooms. In this situation, the geometry of the ‘corridor’ had no influence on the interaction between modes and therefore the system behaved like two similar rooms. If the dimension ratio of the rooms in the z direction were at least an integer value, the panel performance would tend to be quite similar at either position 2 or position 4.

In summary, transmission behaviour becomes complex and dependent on both panel position and panel size. With the panel located at the centre of the common wall, only few structural modes were excited. However, as the panel location was moved into the corner of wall, most of its even and odd modes were excited. This occurred because of the response of a large number of *in vacuo* panel modes to oblique fields excited by the point source.

Another important point is that when the panel-controlled modes are excited below the room-controlled modes, the mass law behaviour may tend to dominate the transmission. However, for the opposite situation, when the panel-controlled resonance frequency is higher than the room-controlled resonance frequency, a non-resonant stiffness behaviour may then dominate. It is also important to mention that SRI is usually inversely proportional to panel size in the non-resonant transmission region. Below the critical frequency, the effect of the panel size is significant when the wall size is entirely flexible. In fact, SRI curves approximate to the mass-law curve.

4.6 - Influence of absorption on SRI parameter

When the modal overlap of rooms is rather low, the cross-modal damping terms (equation 3.4) are generally neglected. In spite of that, the cross-modal terms of the radiation efficiency matrix dominate the resonant contribution, providing that the air is considered a ‘light’ fluid. [18].

According to Figure 7a and 7b, the effect of increasing the absorption coefficient significantly affected the SRI values. For instance, when the reverberation time is decreased, the modal overlap factor is increased and vice-versa. There is a higher probability of better coupling between modes with distinct eigenfrequencies. Therefore, an increase in absorption coefficient for the materials in the receiving room (for both models) led not only to better coupling but also to lower sound insulation at very low frequencies (approximately below 100 Hz). However, when the frequency increased, the modal pressure in the receiving room

(and therefore the transmitted intensity) was significantly reduced for both models. Consequently, the SRI became larger.

4.7 - Influence of source position on the SRI parameter

In this analysis, the whole common wall is used in each model as the elastic structural partition. A point source is placed at the positions shown in Figure 1. Values of SRI obtained for three different source positions are shown in Figures 8a and 8b. The lower value of SRI corresponds to the source located in the middle of the source room, as was expected. With the source situated at this position, only symmetric room modes were excited. In the middle of room, SRI achieved low values compared to the values obtained for the source placed at position 1 (corner) and 2.

For a shallow source room, similar modes are excited in both positions whereas for dissimilar rooms, SRI values may differ due to the coupling with the cubic receiving room (model 2). The three curves tended to differ in the frequency range between 100 and 250 Hz. This reveals that the incident sound field was not yet becoming diffuse. In addition, the performance of panel insulation is generally affected by the power input into the source room. It is also evident that the source position does not alter the coupling factors between the modes of the subsystems [11].

5 Conclusions

A comparison between numerical modal analysis and theoretical predictions has been performed. A narrow bandwidth (0.1 Hz) and a maximum frequency (300 Hz) were used for the frequency response of the systems to a volume velocity point excitation. Above this frequency limit, the computational storage requirements for variables as well as the operational running time on a personal computer became extremely problematic. At the expense of some complexity, the program might be extended to large problems by developing additional routines. The effect of being selective in eliminating some modal contributions has not been considered here. Although there were many 'weak coupling coefficients', it has been shown that their summation were significant to the total coupling. Hence, all possible natural frequencies and their respective modes were included in this analysis.

These results may help the understanding of the model, with a group of subsystems directly related to physical elements such as rooms and flexible partitions. They can also provide an initial discussion for the investigation of a SEA model, which can be useful for practical building acoustics. Although this problem (the coupling between the panel and the acoustic fields) has been solved in previous work by several authors, the main originality of this initial research is to offer guidance on the comprehension of important parameters in a real case of architectural acoustic design. Nevertheless, this is yet to be validated experimentally. All the parameters, which affected the modal composition of the sound field in the subsystems, were fundamental in the determination of the Sound Reduction Index. The results may also be used to predict measurement in-situ at low frequencies, where the classical definition of SRI in ISO140 for diffuse sound fields may not be reliable. Although the assumption of uncoupled 'rigid-walled' acoustic modes for the rooms [6] has been assumed for many years, the boundary condition, which is due to the velocity of the partition, could not be replicated. The convergence problem might be rather sensitive at low frequencies. Hence, the next stage of this research is to develop an alternative model for prediction of noise reduction in terms of Component Mode Synthesis (CMS) method. It will be applied to acoustic-structural coupled rooms.

6 References

1. Ohayon, R. & C. Soize, *Structural Acoustics and Vibration*; Academic Press, UK, 1998.
2. Kroop, W; Pietrzyk, A. & Kihlman, T. *On the meaning of the sound reduction index at low frequencies*, Acta Acustica 2, pp. 379-392, 1994
3. Dowell, E. H., Gorman, G. F., III and Smith, D. A., *Acoustoelasticity: General Theory, Acoustic Natural Modes and Forced response to Sinusoidal Excitation, Including Comparisons with Experiment*, Journal of Sound and Vibration, vol. 52(4), pp. 519-542, 1977.
4. Pan, J., Hansen, C. H. & Bies, D. A., *Active Control of Noise transmission Through a Panel into a Cavity: I. Analytical Study*, J. Acoust. Soc. Am. vol 87(5), pp. 2098-2108, 1990.
5. Kim, S. M. & Brennan M. J., *A Compact Matrix Formulation Using the Impedance and Mobility Approach for the Analysis of Structural-Acoustic Systems*, Journal of Sound and Vibration, vol. 223(1), pp. 97-113, 1999.
6. Fahy, F. J., *Sound and Structural Vibration*, Academic Press, U.K., 1985.
7. Takahashi, D.; *Effects of panel boundedness on sound transmission problems*; J. Acoust. Soc. Am. 98(5), pp. 2598-2606, 1995.
8. Guy, R. W. & Bhattacharya; *The transmission of sound through a cavity-backed finite plate*; Journal of Sound and Vibration, 27(2) pp. 207-223, 1973.
9. Craik, R. J. M.; *Sound Transmission Through Buildings using Statistical Energy Analysis*; Gower Publishing Limited, U.K., 1996.
10. Osipov, A., Mess, P. and Vermeir, G.; *Low-Frequency Airborne Sound Transmission Through Single Partitions in Buildings*; Applied Acoustics, vol. 52, no. 3-4, pp. 273-288, 1997.
11. Maluski, S. and Gibbs, B. , *The influence of partition boundary conditions on sound level difference between rooms at low frequencies*, Euro noise 98, pp. 681-685, 1998.
12. Maluski, S. and Gibbs, B.; *Sound Insulation between dwellings at low frequencies using a Finite Element Method*. Proc. I. O. A. vol22, part 2, 2000.
13. Gagliardini, L. & Roland, J.; *The Use of a Functional Basis to Calculate Acoustic Transmission Between Rooms*; Journal of Sound Vibration, 145(3), pp. 457-458, 1991.

14. A. D. Pierce, *Acoustics: An Introduction to its Physical Principles and Applications*, New York: McGraw-Hill, 1981.
15. White, F. M.; *Fluid Mechanics*, McGraw-Hill International Editions, Fourth Edition, Singapore, 1999.
16. Beranek, L. L. & Vér, I. L., *Noise and Vibration Control Engineering*, John Wiley & Sons, Inc. USA, 1992.
17. Maidanik, G.; *Response of Ribbed Panels to Reverberant Acoustic Fields*, J. Acoust. Soc. Am.; vol 34, no. 6, pp. 809-826, 1962.
18. Leppington, F.G., Heron, K. H., Broadbent, F. R. S., & Mead, S. M., *Resonant and Non-Resonant Acoustic Properties of elastic Panels. II. The transmission Problem*, Proc. Roy. Soc. Lond., A 412, pp. 309-337, 1987.
19. Leppington, F., Broadbent, E., & Heron, K., *The acoustic radiation efficiency of rectangular panels*, Proc. Roy. Soc. Lond., A 382, pp. 245-271, 1982.
20. Dowell, E. H.; *Reverberation Time, Absorption, and Impedance*; J. Acoust. Soc. Am.; vol 64(1), pp. 181-191, 1978.
21. Beranek, L. L.; *Noise and Vibration Control*; McGraw-Hill Book Company, 1971.
22. Kuttruff, H. ;*Room acoustics*; Spon press, 4th Edition, U.K., 2000.

7 Tables

The natural frequencies of the first 10 room modes			
Number of modes = 90		Number of modes = 39	
Room 1(2x2x5) m ³	Frequency	Room 2 -(2x2x2) m ³	Frequency
Mode (l,m,n)	(Hz)	Mode (l,m,n)	(Hz)
0 0 0	0.00	0 0 0	0.00
0 0 1	34.00	0 0 1	85.00
0 0 2	68.00	0 1 0	85.00
0 1 0	85.00	1 0 0	85.00
1 0 0	85.00	0 1 1	120.21
0 1 1	91.55	1 0 1	120.21
1 0 1	91.55	1 1 0	120.21
0 0 3	102.00	1 1 1	147.22
0 1 2	108.85	0 0 2	170.00
1 0 2	108.85	0 2 0	170.00

Table 1: Summary of the natural frequencies of 'rigid-wall' acoustic volumes

Panel modes Dimension: (1x1) m ²		First 08 panel modes Dimension:(2x2) m ²		First 08 panel modes Dimension: (2x5) m ²	
Mode (p,q)	Frequency (Hz)	Mode (p,q)	Frequency (Hz)	Mode (p,q)	Frequency (Hz)
1 1	37.88	1 1	9.47	1 1	5.49
1 2	94.69	1 2	23.67	1 2	7.76
2 1	94.69	2 1	23.67	1 3	11.55
2 2	151.51	2 2	37.88	1 4	16.86
1 3	189.39	1 3	47.35	2 1	19.70
3 1	189.39	3 1	47.35	2 2	21.97
2 3	246.20	2 3	61.55	1 5	23.67
3 2	246.20	3 2	61.55	2 3	25.76

Table 2: Summary of the *in vacuo* natural frequencies of partitions used into the models.

First 10 natural frequencies (model 1) Panel dimension: (2 x 5) m ²		First 10 natural frequencies (model 2) Panel dimension: (2 x 2) m ²	
Coupled Frequency	Coupled frequency (damping included)	Coupled Frequency	Coupled frequency (damping included)
0.0000	0.0000	0.0000	0.0000
7.2641	7.2639	12.5531	12.5427
10.0209	10.0236	23.1829	23.1827
13.1633	13.1529	23.1999	23.1996
16.4268	16.4267	34.3852	34.3821
19.2544	19.2541	37.4325	37.4321
21.5426	21.5423	46.9924	46.9918
23.4503	23.4498	47.1532	47.1525
25.3602	25.3599	61.0946	61.0939
30.6787	30.6783	61.1387	61.1379

Table 3: Summary of the first 10 coupled natural frequencies of model 1 and 2

First 10 natural frequencies of model 1 - Panel dimension-(1 x 1) m ²					
F _{c1} (Hz)	F _{dc1} (Hz)	F _{c2} (Hz)	F _{dc2} (Hz)	F _{c3} (Hz)	F _{dc3} (Hz)
0.0000	0.0000	0.0000	0.0000	0.0000	0.0000
32.9489	32.9491	33.5497	33.5488	33.9988	33.9955
33.9999	33.9967	34.0000	33.9967	34.0000	33.9967
38.4513	38.4473	38.0286	38.02570	37.4711	37.4706
68.0000	67.9984	68.0000	67.9984	68.0000	67.9984
68.1311	68.1295	68.0049	68.0032	68.2140	68.2124
84.9693	84.9674	84.9353	84.9334	84.9177	84.9158
84.9999	84.9981	84.9999	84.9981	85.0000	84.9981
85.0000	84.9981	85.0000	84.9981	85.0000	84.9981
85.2046	85.2026	85.1686	85.1666	85.1581	85.1562

Table 4: Summary of the coupled natural frequencies - panel at positions 1, 2 and 3-

Natural frequencies: F_c - coupled freq; F_{dc} - coupled damped frequencies.;

First 10 natural frequencies of model 2 -Panel dimension-(1 x 1) m ²					
F _{c1} (Hz)	F _{dc1} (Hz)	F _{c3} (Hz)	F _{dc3} (Hz)	F _{c5} (Hz)	F _{dc5} (Hz)
0.0000	0.0000	0.0000	0.0000	0.0000	0.0000
33.4195	33.4190	33.5849	33.5838	33.7592	33.7575
38.0269	38.0235	38.1341	38.1313	37.7291	37.7268
68.0651	68.0634	68.0024	68.0008	68.0022	68.0006
84.9361	84.9432	84.8567	84.8686	84.9364	84.9434
84.9639	84.9673	84.8977	84.8951	84.9642	84.9675
85.0000	84.9845	85.0000	84.9836	84.9999	84.9846
85.0000	84.9998	85.0000	85.0055	84.9999	84.9998
85.4459	85.4393	85.2729	85.2628	85.4513	85.4448
91.4461	91.4444	91.3872	91.3855	91.5051	91.5031

Table 5: Summary of the coupled natural frequencies - panel at positions 1, 3, and 5 -

Natural frequencies: F_c - coupled freq.; F_{dc} - coupled damped freq.;

8 Figures

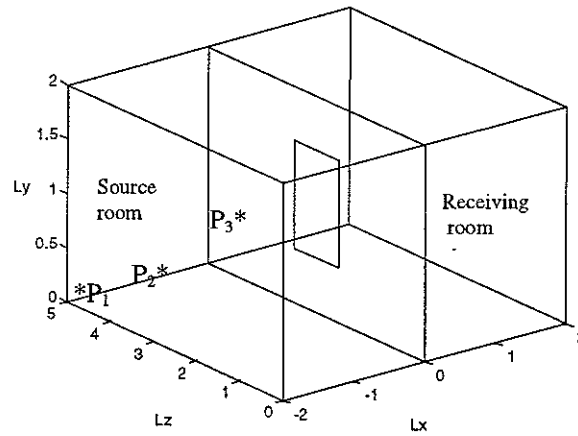


Figure 1: Two rooms separated by a common wall with a centered flexible panel.

Coordinates of the point sources : $P_1 = (-2,0,0)$ – at the corner ; $P_2 = (-1,0,0)$

$P_3 = (-1,1,2.5)$ – In the middle of the room

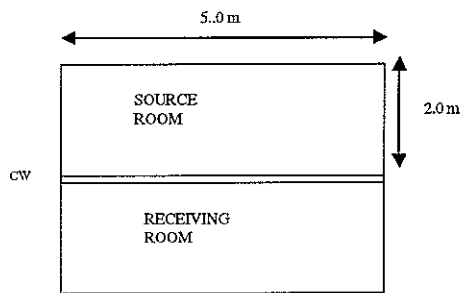


Figure 2a: Model 1 with identical rooms
(Height=2.0m)

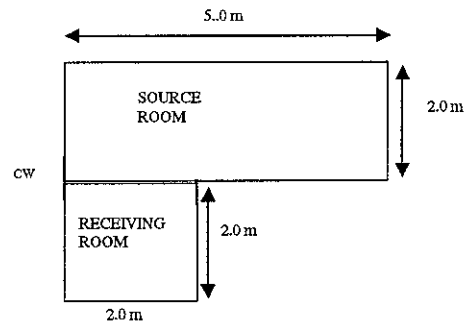


Figure 2b: Model 2
(Height = 2.0 m)

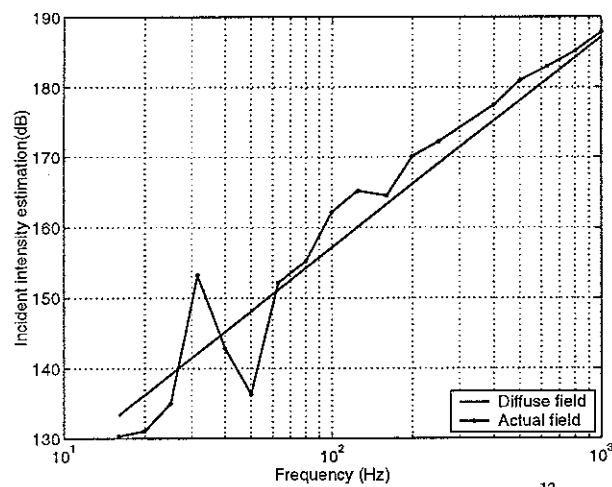


Figure 3: Prediction of the incident intensity on the panel. (dB re 10^{-12} W/m²) – 1/3 octave band

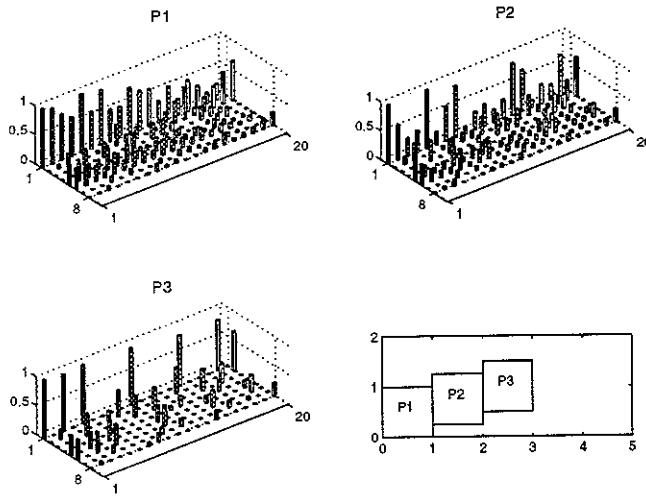


Figure 4a: Normalized coupling coefficients for panel at positions P1-P3 and source room - Model 1 (8 panel modes and 90 room modes) - 1/3 octave band

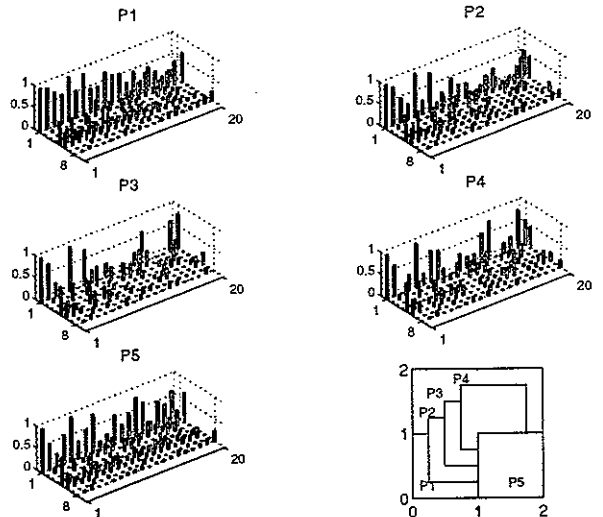


Figure 4b: Normalized coupling coefficients for panel at positions P1-P5 and source room - Model 2 (39 receiving room modes) - 1/3 octave band

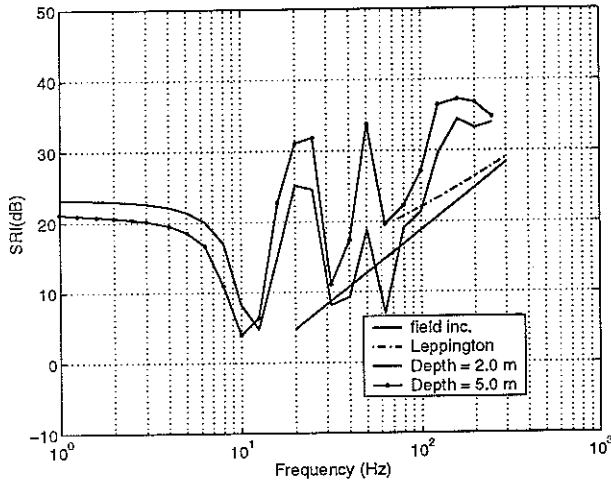


Figure 5a: The effect of source room depth on SRI for model 1 - common wall ($2 \times 5 \text{ m}^2$) - 1/3 octave band

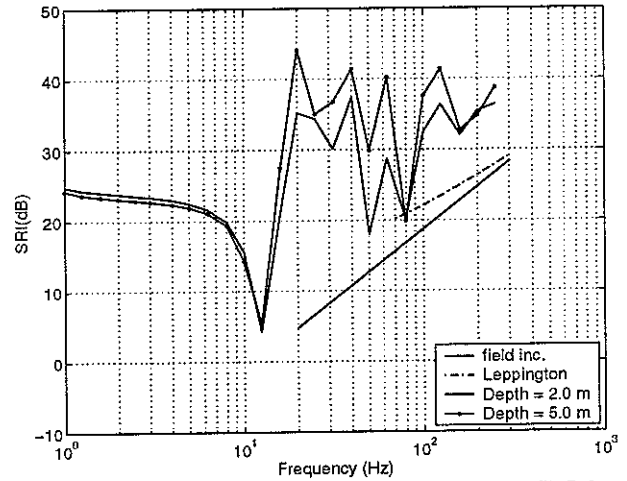


Figure 5b: The effect of source room depth on SRI for model 2 - common wall ($2 \times 2 \text{ m}^2$) - 1/3 octave band

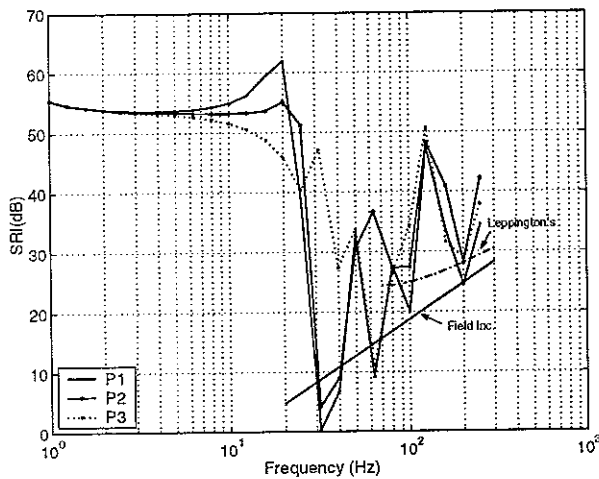


Figure 6a: The effect of different panel positions in the common wall on SRI - Model 1 - 1/3 octave band

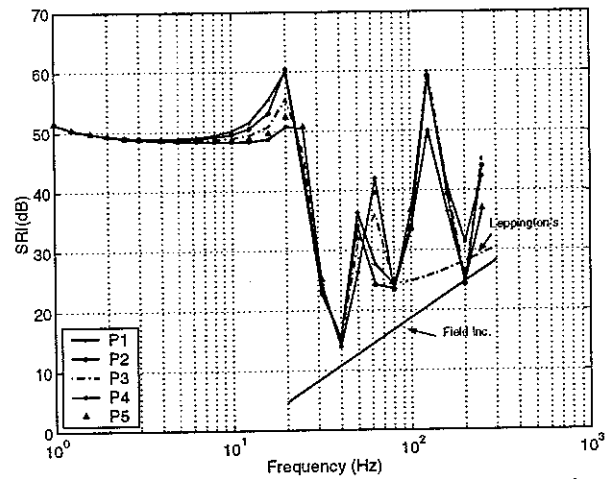


Figure 6b: The effect of different panel positions in the common wall on SRI - Model 2 - 1/3 octave band

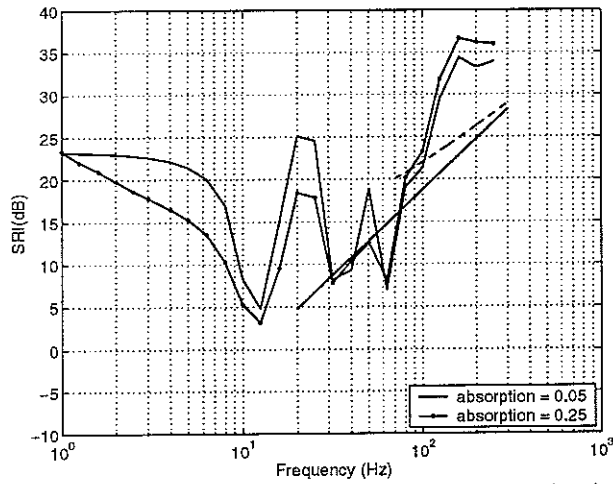


Figure 7a: The effect of the increasing of absorption in the receiving room on SRI - model 1 - 1/3 octave band

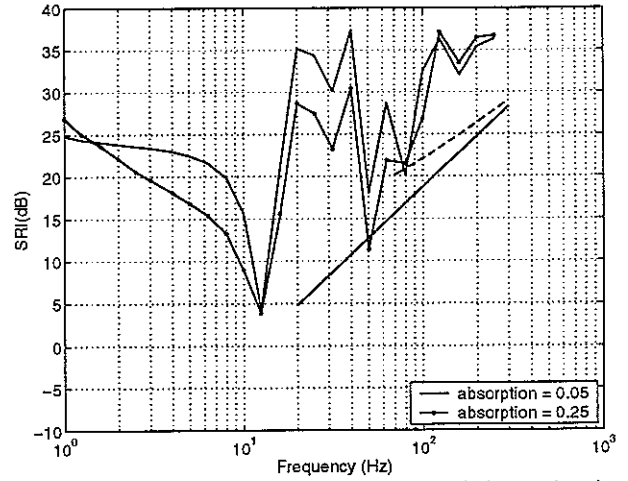


Figure 7b: The effect of the increasing of absorption in the receiving room on SRI - model 2 - 1/3 octave band

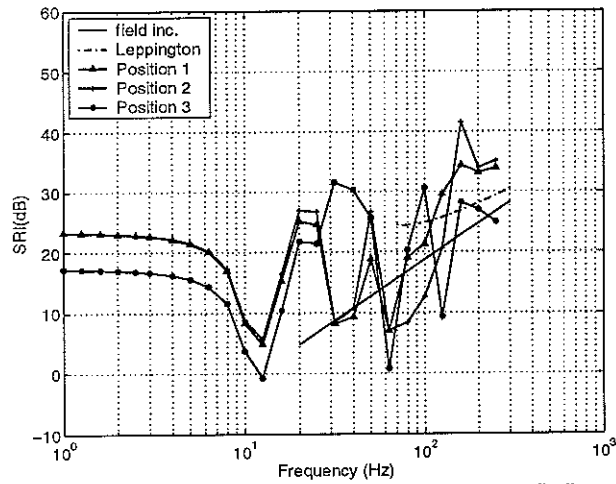


Figure 8a: The effect of source position on SRI considering the whole flexible panel ($2 \times 5 \text{ m}^2$)- model 1 - 1/3 octave band

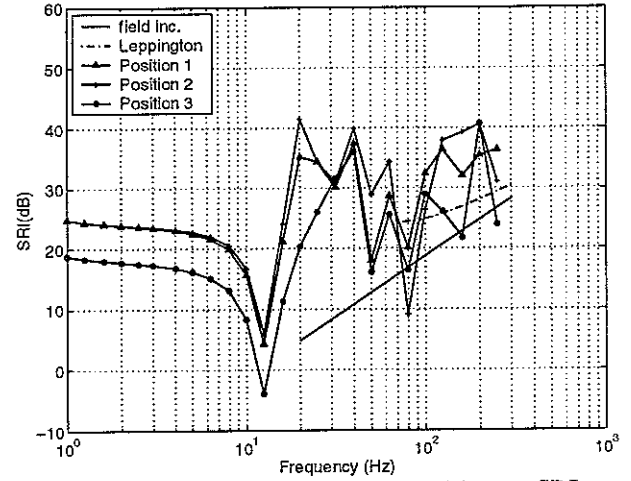


Figure 8b: The effect of source position on SRI considering the whole flexible panel ($2 \times 2 \text{ m}^2$)- model 2 - 1/3 octave band

9 Appendix - List of symbols

- c_o - ambient (equilibrium) speed of sound;
 $p(z,y,0)$ - Pressure over the panel surface;
 k_z - trace wavelength of the panel at the z direction;
 k_y - trace wavelength of the panel at the y direction;
 k_b - trace wavelength of free-bending waves propagating in a infinite panel;
 k_{pr} - trace wavelength of the panel *in vacuo*;
 w - normal displacement of the panel surface;
 C_{n1p} - geometrical coupling between the source room and the panel;
 C_{n2p} - geometrical coupling between the receiving room and the panel;
 F_n^R - generalized force exerted on the p^{th} plate mode by the n^{th} acoustic mode of the receiving room;
 $G(\mathbf{r}|\mathbf{r}_o)$ - Green's Function – solution to equation (2.14);
 P_n^R - receiving room modal pressure;
 Q_n - generalized volume velocity; see equation (3.3);
 Z_a - real specific acoustic impedance; see equation (3.5);
- α - constant diffuse absorption coefficient;
 β_p, β_n - Modal damping parameter of the panel and of the acoustic space respectively;
 ϕ_p, ϕ_q - function basis for the eigenfunctions of a simply-supported plate;
 η - Internal loss factor;
 ρ_o - density of air (equilibrium);
 τ - transmission efficiency – see equation (2.1);
 ω - forced angular frequency;
 ψ_n - function basis for the mode shapes of an acoustic volume boundary by rigid walls;
 $\Pi(\omega)$ - Power radiated into a half-space due to the plate vibration in the frequency domain;
 ∇ - Laplace's operator;
 $\Phi_{n1,n2}$ - Potential velocity function corresponding to the source and receiving rooms;
 Λ_p - Generalized modal mass for the panel;
 Λ_n - Generalized modal mass for the the acoustic volume;